IEEE SENSORS 2012

Taipei International Convention Center - October 28-31, 2012 - Taipei, Taiwan

Tutorials: 28 October 2012; Conference: 29-31 October

Sponsored by the IEEE Sensors Council, www.ieee-sensors.org

"You know, yesterday at a session I heard a couple interesting ideas that I will definitely try now in my lab. If I hadn't come here - I usually go to my society's Conference on Chemical Sensors – I wouldn't have learned those things. This conference is so good in this respect – it connects people from different communities with interests in sensing."
--From a coffee break conversation at the IEEE SENSORS 2011 Conference, Limerick, Ireland

NAVIGATION

- IEEE SENSORS 2012
- LOCAL ORGANIZERS/SPONSOR
- ORGANIZING COMMITTEE
- KEYNOTE SPEAKERS
- TPC MEMBERS
- PROGRAM
- AUTHORS
- SPECIAL SESSIONS
- TUTORIALS
- SOCIAL EVENTS
- REGISTRATION
- EXHIBITS/PATRONS
- HOTELS
- TRAVEL/LOCAL INFO
- VENUE
- LOCAL ATTRACTIONS
- CONTACT US

IEEE SENSORS 2012

Register Online

IEEE SENSORS 2012 is intended to provide a forum for research scientists, engineers, and practitioners throughout the world to present their latest research findings, ideas, and applications in the area of sensors and sensing technology. IEEE SENSORS 2012 will include keynote addresses and invited presentations by eminent scientists.

Read more »

Photography Policy and Non-Discrimination Policy

Event Photography Statement

No photography or video recording is permitted during the sessions. Photography or video of posters is allowed only with the permission of the authors.

Attendance at, or participation in, this conference constitutes consent to the use and distribution by IEEE of the attendee's image or voice for informational, publicity, promotional and/or reporting purposes in print or electronic communications media. No flash photography will be used.

Read more »

Exhibition and Patron Opportunities

The Organizing Committee for the IEEE SENSORS 2012 Conference would like to invite you to participate as a supporter and/or exhibitor at the upcoming Conference to be held 28-31 October 2012 in Taipei, Taiwan.

The IEEE Sensors Council's conference on Sensors is the authoritative meeting focusing on interdisciplinary research topics for the exchange of information regarding research and development in Sensors and its related fields.

Read more »

IMPORTANT DATES

21 May 2012	Abstract Submission Deadline
10 Aug 2012	Final Full Paper Submission (4 Pages)
10 Aug 2012	Presenting Author and Early-Bird Registration Deadline

Monday Poster Session Session

Session Type: Poster
Session Code: A4P-G
Location: Room 201
Date & Time: Monday October 29, 2012 (15:00 - 16:50)
Chair: Pin Chang,
Wen-Pin Shih

Add To My Sched	Paper Id	Topic	Title / Author
☐	1024	1	Advanced Technique to Suppress Subject Variability for Bio-Impedance Based Alcohol-Intake Detection *Kazuma Kojima, Susumu Tamura, Yasuhisa Omura*
☐	1245	1	Study on Flow Behavior of BCB in Adhesive Bonding Aiming at Reducing Transverse Deformation *Kangfa Deng, Huan Zheng, Shaobo Jiang, Wei Zhang*
☐	1512	1	RF Tomography: Self Calibration of Distributed RF Sensors *Lorenzo Lo Monte, Russell Vela, Michael Wicks*
☐	1598	1	Temperature Influence Investigation on Hall Effect Sensors Performance Using a Lumped Circuit Model *Maria-Alexandra Paun, Jean-Michel Sallese, Maher Kayal*
☐	1600	1	Electrostatic Levitation: Analysis and Dependence on Comb-Drive Parameters *Anindya Lal Roy, Tarun Kanti Bhattacharyya*
☐	1792	1	Modeling the Sensing Behavior of a MEMS Field Ionization Device Coupled with Capacitive Actuation *Thomas Walewyns, Laurent Francis*
☐	1032	2	Love Wave Devices with Excellent Temperature Stability for Application in Gas Sensor *Wen Wang, Xiao Xie, Jiaoli Hou, Shitang He*
☐	1054	2	Development of Methanol Sensor Using Shear Horizontal Surface Acoustic Wave Devices for Direct Methanol Fuel Cells *Sabro Endo, Takuya Nozawa, Jun Kondoh*
☐	1055	2	Hydrogen Sensors Based on GaN Diodes: the Sensing Mechanism *Yoshihiro Irokawa*
☐	1074	2	Electrodeposited Pd/Ni/Si Micro-Channel Plate Electrode for Hydrogen Peroxide Detection and Application *Yuzhu Jing, Bobo Peng, Tao Liu, Fei Wang, Lianwei Wang, Paul K Chu*
☐	1240	2	A Highly Fast Capacitive-Type Humidity Sensor Using Percolating Carbon Nanotube Films as a Porous Electrode Material *Hyun Pyo Hong, Kyung Hoon Jung, Nam Ki Min, Yong Hoon Rhee, Chan Wo...*
☐	1326	2	Development of a Multichannel Taste Sensor Chip for a Portable Taste Sensor *Yusuke Tahara, Yoshihiro Maehara, Ji Ke, Akihiro Ikeda, Kiyoshi Tok...*
☐	1363	2	A Capacitive Relative Humidity Sensor Using Polymer Nanoparticles *Yifan Wang, Mohamadsadegh Hajhashemi, Behraad Bahreyni*
☐	1416	2	Ethanol Sensing Characteristics of Sensors Based on ZnO:Al Nanostructures Prepared by Thermal Oxidation *Supab Choopun, Duangmanee Wongratanaphisan, Atcharawon Gardchareon,...*
☐	1447	2	Determination of Total Phosphorus in Water Environment by Three-Dimensional Double Coils Microelectrode Chip *Qiannan Xue, Chao Bian, Jianhua Tong, Jizhou Sun, Hong Zhang, Shanh...*
☐	1462	2	Setup and Properties of a Fully Inkjet Printed Humidity Sensor on PET Substrate *Eric Starke, Alexander Türke, Marion Schneider, Wolf-Joachim Fische...*
☐	1664	2	Gravure Printed Surface Enhanced Raman Spectroscopy (SERS) Substrates for Detection of Toxic Heavy Metal Compounds *Ali Eshkeiti, Avuthu Sai Guruva Reddy, Binu Baby Narakathu, Margare...*
☐	1059	4	Plastic Optical Fiber Microbend Sensor Used as Breathing Sensor *Zhihao Chen, Ju Teng Teo, Soon Huat Ng, Xiufeng Yang*
☐	1110	3	Development of an Implantable Micro Temperature Sensor Fabricated on the Capillary for Biomedical and Microfluidic Monitoring *Zhuoqing Yang, Yi Zhang, Toshihiro Itoh*
☐	1147	3	A High Sensitivity Chemiluminescence-Based CMOS Image Biosensor for the Detection of Human Interleukin 5 (IL-5) *Hyou-Arm Joung, Dong-Gu Hong, Min-Gon Kim*
☐	1159	3	Evaluation of Antioxidant Activity Using CNT Electrode by Detecting Hydroxyperoxides on Oxidized LDL *Futaba Ohkawa, Seiji Takeda, Shu-Ping Hui, Toshihiro Sakurai, Hirot...*
☐	1162	4	Silicon-Based Guided-Wave Optical Accelerometer: Experimental Consideration to Establish its Design Guideline

Information for Paper ID 1074

Paper Information:

Paper Title:	Electrodeposited Pd/Ni/Si Micro-Channel Plate Electrode for Hydrogen Peroxide Detection and Application
Student Contest:	Yes
Affiliation Type:	Academia
Keywords:	Hydrogen peroxide sensor Micro-channel plate Palladium nanoparticle Cyclic voltammetry Amperometric detection
Abstract:	A sensor based on Pd/Ni/Si micro-channel plate electrode was fabricated by electrochemical deposition method of chronopotentiometry for the detection of H2O2. The morphology and structure of the electrode were characterized by XRD and SEM. The electrochemical behavior of the H2O2 sensor was also investigated by cyclic voltammetric and amperometric techniques in the 0.1 mol/L KOH solution. The Pd/Ni/Si MCP electrode exhibited high electrocatalytic activity in the oxidation of H2O2. Under the optimal conditions, the linear relationship between catalytic current and time was obtained and the correlation coefficient was 0.99923. The prepared electrode exhibited an ultrahigh sensitivity. In addition, the electrode possessed superior stability, anti-interference and selectivity. These results indicate that a sensor based on the Pd/Ni/Si MCP electrode is suitable for detection of H2O2. Further work is in progress.
Track ID:	2
Track Name:	Chemical and Gas Sensors
Final Decision:	Accept as Poster
Session Name:	Monday Poster Session (Poster)

Electrodeposited Pd/Ni/Si micro-channel plate electrode for hydrogen peroxide detection and application

Y.Z. Jing, B.B. Peng, T. Liu, F. Wang , L.W. Wang
Laboratory of Polar Materials and Devices, MOE
and Department of Electronic Engineering
East China Normal University
Shanghai, China
e-mail: lwwang@ee.ecnu.edu.cn

Paul K. Chu
Department of Physics and Material Sciences,
City University of Hong Kong,
Tat Chee Avenue, Kowloon, Hong Kong, China

Abstract—**A novel method to construct a sensitive amperometric sensor for hydrogen peroxide(H_2O_2) is described. It is composed of highly dispersed palladium nanoparticles on a vertically aligned nickel-coated silicon micro-channel plate (MCP). The morphology of the Pd/Ni/Si-MCP electrode is characterized by scanning electron microscopy (SEM) and X-ray diffraction (XRD). The electrode with a three-dimensional structure shows high-catalytic activity towards oxidation of H_2O_2 in a 0.10 M KOH solution. The electrode boasts a high sensitivity of 0.86 mAmM-1cm^{-2} at an applied potential of 0.12V, and the detection limit is 7.6 μM. The linear range is up to 12.5mA with a linear correlation of 0.99923. In addition, the electrode also exhibits superior stability, anti-interference, and selectivity. These features demonstrate the Pd/Ni/Si-MCP electrode is suitable for detection of H_2O_2.**

I. INTRODUCTION

A high-sensitivity H_2O_2 sensor is very important to food, pharmaceutical, and environmental analysis, as well as research of underwater power metal semi fuel cells or cathode oxidants of direct borohydride fuel cells. Currently, several analytical techniques including titration [1], fluorescence [2], chemiluminescence[3], spectrophotometry [4] and electrochemistry [5,6] have been applied to the determination of H_2O_2. Among them, electrochemical analysis has been widely used due to several advantages that include fast response, high sensitivity and perfect selectivity.

In general, there are two different types of electrical H_2O_2 sensors, which are based on whether or not the working electrode is immobilized with an enzyme. The enzyme-modified electrode has been primarily studied due to its high catalytic activity and excellent selectivity [7,8]. However, the enzyme-modified electrode requires a relatively harsh environment for its application and storage. To overcome these obstacles, more attention has been paid to non-enzymatic H_2O_2 sensors.

Until now, various materials of metal nanoparticles or thin films have been reported, but improving the response of nonenzymatic H_2O_2 sensors to attain excellent sensitivity is still a big challenge. Typically, the sensing properties of amperometric sensors strongly depend on the effective surface area of the electrode materials. The application of three-dimensional materials to the design of H_2O_2 sensors is currently an active research area and variety of three-dimensional structures have attracted interests because of their unique properties which differ from those of traditional bulk materials. In this work, an ordered silicon micro-channel plate (MCP) was employed as the backbone of the electrode in an H_2O_2 sensor. The silicon MCP structure was fabricated by photo-assisted electrochemical etching [9,10]. The novel structure boasts a large surface-to-bulk ratio, high loading of catalysts and good mechanical stability. The high porosity and appropriate geometry of the three-dimensional array reinforce mass transport and catalytic effect, thus playing an important role in fast electron transfer in the electrode reactions during H_2O_2 detection. Our experimental results confirm that the ordered macro-porous electrode has high sensitivity and offers a low detection limit, wide linear range, and good long-term stability. The excellent analytical performance confirms the applicability of this composite electrode in non-enzyme H_2O_2 sensing.

II. EXPERIMENTAL

A. Chemicals

The wafer used to fabricate the MCP was single-sided, polished, p-type silicon with a resistivity of 2-9 Ωcm and a thickness of 525 μm. Hydrofluoric acid, hydrochloric acid, palladium dichloride, hydrogen peroxide, and the other reagents were of analytical reagent grade and used without further purification. The aqueous solutions were prepared with 18 MΩ de-ionized water. All the experiments were carried out at room temperature in a clean environment.

B. Preparation of the Pd/Ni/Si MCP electrode

1) Silicon MCP Preparation

This work was jointly supported by Shanghai Foundamental Key Project No. 11JC1403700, , PCSIRT, the National Natural Science Foundation of China (No. 61176108), and Hong Kong Research Grants Council (RGC) General Research Funds (GRF) No. CityU 112510.

One 100mm in diameter, p-type, <100> oriented, 2-9Ω·cm silicon wafer with a thickness of 525 μm was used in our experiments. A silicon dioxide layer (300nm thick) was formed by thermal oxidation as a masking layer. Patterned by a standard photolithographic process, windows 3 μm x 3 μm square lattices were opened. Then the patterned wafer was pre-etched in a 25 wt% tetramethyl ammonium hydroxide (TMAH) aqueous solution at 85°C to form the pits with a shape of an inverted pyramid. After anodization by photo-assisted electrochemical etching, the silicon MCP was formed [9,10]. The thickness of the silicon MCP was about 200 μm with pores about 5 μm x 5 μm and wall about 1 μm.

1) Preparation of nickel-coated silicon micro-channel plate(MCP) electrode

Because the etching process degraded the electrical conductivity of the silicon MCP, a thin nickel film was produced on the surface of the MCP by electroless deposition to serve as the electrically conductive layer. To enhance adhesion between the Ni layer and silicon surface, the sample was treated in a solution (40% hydrofluoric acid: ethanol: deionized water: Triton X-100=130: 70: 100: 2, v: v) for 5 min. Electroless deposition was carried out and the details regarding the electroless deposition can be found in our previous work [11]. In order to further improve the surface area and conductivity of the Ni/Si-MCPs, the structure of the porous nano-Ni was created by the electrochemical nickel-plated method. Electrodeposition of the porous nano-Ni film was performed in a standard two-electrode glass cell at 23±1 °C using an electrolyte consisting of 2 M NH_4Cl and 0.1 M $NiCl_2$ at a pH value of 3.5, a clean Ni/Si-MCPs as the working electrode, and a Pt foil as the counter electrode. The distance between the two electrodes was 1 cm, and the electrodeposition was carried out at a constant current of 0.25 A cm^2 for 90 s.

2) Preparation of Pd/Ni/Si micro-channel plate electrode

The silicon MCP was then put into a buffer solution of Triton X-100 for at least 2 minutes to increase the hydrophilicity. Afterwards, the Pd/Ni/Si MCP electrode were created by the electrochemical palladium-plated method. Electrodeposition by chronoamperometry of palladium nanoparticles was also performed in a standard two-electrode glass cell at 23±1 °C. Electrodeposition was carried out at a current density of 0.6 m A /cm^2 for 100 s in a mixture of 0.096 mM $PdCl_2$ and 0.005 M HCl. PdC_{l2} was used as the metal ion source. The working electrode was a nickel-coated silicon micro-channel plate prepared before and the other was a Pt foil as the counter electrode. Afterwards, the Pd/Ni/Si MCP electrode was washed with de-ionized water several times. Then it was rapid thermal annealed at 400°C for 60s under argon. The electrode transverse area was approximately 0.25 cm^2.

C. Apparatus and characterization

The morphology and microstructure were examined by scanning electron microscopy (SEM, JSM 5610). The deposited materials were characterized by X-ray diffraction (XRD) using Cu Kα radiation. The electrochemical properties of the Pd/Ni/Si MCP were determined by cyclic voltammetry (CV) and amperometry. Electrochemical measurements were carried out on a three-electrode electrochemical working station (Shanghai Chenhua CHI660D) with a saturated calomel electrode and platinum gauze electrode serving as the reference electrode and counter electrode, respectively. All the potentials were referenced to the SCE reference electrode.

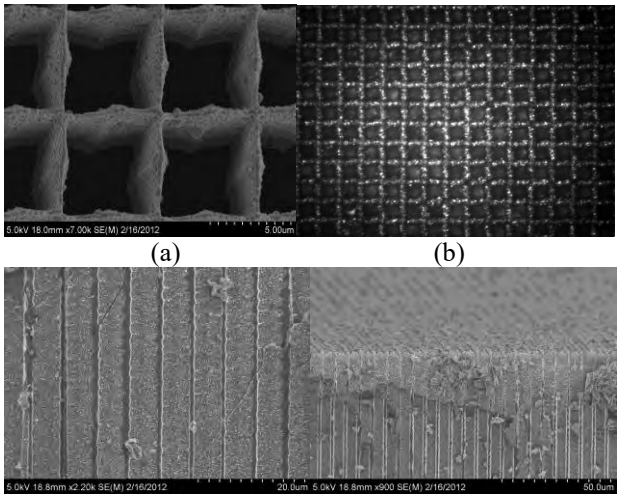

Fig. 1 (a) SEM image of the Ni-MCP sample(top view);
(b) Image magnified 400 times of Pd/Ni/Si MCP;
(c) Cross section of Pd/Ni/Si MCP electrode;
(d) SEM image of the cross section of Pd/Ni/Si MCP electrode.

III. Results and Discussion

A. Characterization of the Pd/Ni/Si MCP electrode

Figs. 1 and 2 show the characterization results of the Ni/Si MCP electrode and Pd/Ni/Si MCP electrode. The SEM data reveal the basic structural characteristics of the three-dimensional array which has good surface quality and can increase the active sites than the planar electrode. Fig. 1(c) depicts the surface topography of the cross section of the Pd/Ni/Si MCP structure. An additional layer can be observed on the surface of the MCP. The structure of the layer is characterized by X-ray diffraction in Fig. 2 which shows the characteristic peaks of crystalline Pd at 40.12° and 46.66° corresponding to the (111) and (200) planes, respectively.

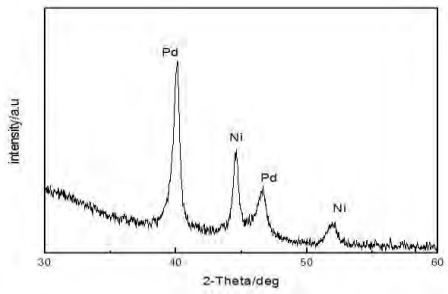

Fig. 2 X-ray diffraction pattern of the Pd/Ni/Si MCP electrode.

B. *Electrocatalytic oxidation of H_2O_2 by palladium nanoparticles*

The electrocatalytic activity of the Pd/Ni/Si MCP electrode towards the oxidation of H_2O_2 under alkaline conditions is studied by cyclic voltammetry. The cyclic voltammogramms acquired from the Pd/Ni/Si MCP electrode in the absence and presence of 5 mM H_2O_2 in a 0.1M KOH solution at a scanning rate of 100 mV/s are shown in Fig. 3. When hydrogen peroxide has electrochemical oxidation on the Pd/Ni/Si MCP electrode, there is an obvious oxidation peak at 0.12 V. The potential decreases obviously and the current increases, indicating that the modified Pd/Ni/Si MCP electrode catalyzes oxidation of hydrogen peroxide. Fig. 3 also shows that the electrode has catalytic activity on hydrogen peroxide oxidation and reduction, but the electrocatalytic oxidation activity is more obvious than the reduction one.

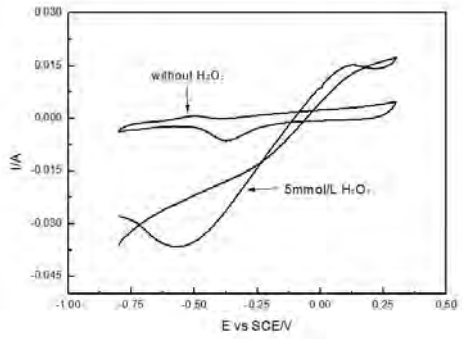

Fig. 3 Cyclic voltammograms obtained from the Ni/Si MCP electrode in the absence and presence of 5 mmol/L H_2O_2 in a 0.1 M KOH solution at a scan rate of 100 mV/s.

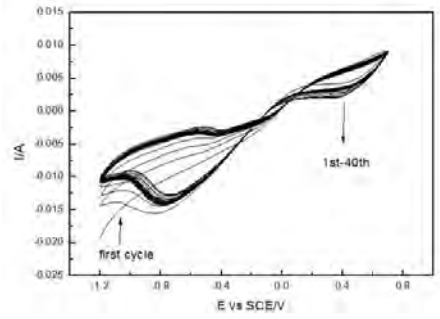

Fig. 4 Cyclic voltammograms of the Pd/Ni/Si MCP electrode in the presence of 5 mmol/L H_2O_2 in a 0.1M KOH solution at scan rate of 100 mv/s for 40 cycles.

Fig. 4 is the cyclic voltammograms of the Pd/Ni/Si MCP electrode in the presence of 5 mmol/L H_2O_2 in .1M KOH at scanning rate of 100 mV/s for 40 cycles, indicating that the electrode has good repeatability and stability.

In order to investigate the role of palladium particles in the catalytic oxidation of H_2O_2, the CV of the Ni/Si MCP electrode obtained in a blank solution and after addition of H_2O_2. Similar to that shown in Fig.5, it has catalytic effects in the decomposition of H_2O_2, but the oxidation current is smaller. The oxidation potential is higher than that of the Pd/Ni/Si MCP. This analysis is also applicable to the reduction peak current. These phenomena indicate that Pd plays an important role in the electrocatalytic oxidation of H_2O_2.

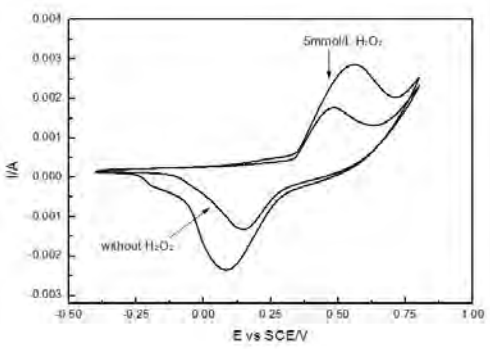

Fig. 5 Cyclic voltammograms acquired from the Ni/Si MCP electrode in the absence and presence of 5 mmol/L H_2O_2 in a 0.1 M KOH solution at a scan rate of 100 mV/s.

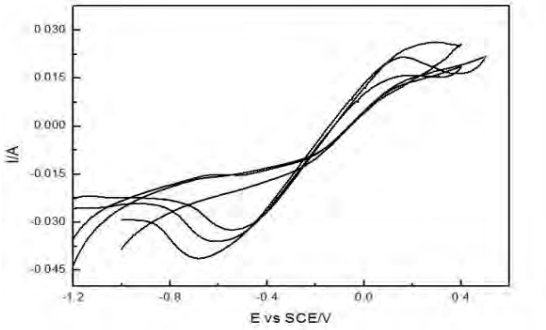

Fig. 6 Cyclic voltammograms of a 0.1M KOH solution containing 5mMH_2O_2 at different scan rate from 20-100 mv/s.

Fig. 6 shows the cyclic voltammograms of the sensor in a 0.1 M KOH solution containing 5 mM of H_2O_2 at different scanning rates from 20-100 mV/s. The anodic peak current is proportional to the square root of the scanning rate. A good linearity between the square root of the scanning rate and peak current can be observed in the range of 20-100 mVs^{-1}, as demonstrated in Fig. 7. The correlation coefficient is 0.99991, indicating that the electrocatalytic oxidation kinetics is mainly controlled by diffusion of H_2O_2 in the solution. The current response at 0.12 V is ideal for quantitative determination of H_2O_2.

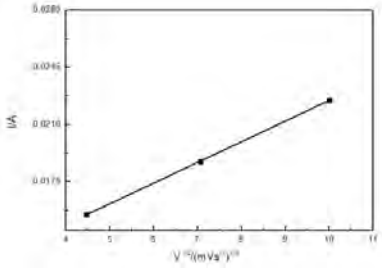

Fig. 7 Dependence of the oxidation peak current on the potential scanning rates.

C. *Sensitivity and linearity*

The amperometric response of H_2O_2 on the Pd/Ni/Si MCP electrode is measured in 0.1 M KOH by continuous addition of H_2O_2 under stirring at a fixed potential of 0.12 V, as shown in Fig. 8. Fig. 9 shows the calibration curve of the response current as a function of time. In the concentration range from 2.5 mM to 12.5 mM with a detection limit of 7.6 μM, the current varies linearly with the H_2O_2 concentration with a correlation coefficient is 0.99923. The Pd/Ni/Si MCP electrode exhibits a high sensitivity of 0.86 $mAmM^{-1}cm^{-2}$. The results indicate that the Pd/Ni/Si MCP electrode has higher sensitivity and a wide linear range compared to before. It results from two indispensable factors, namely the high catalytic activity of the palladium nanoparticles and framework by the silicon MCP.

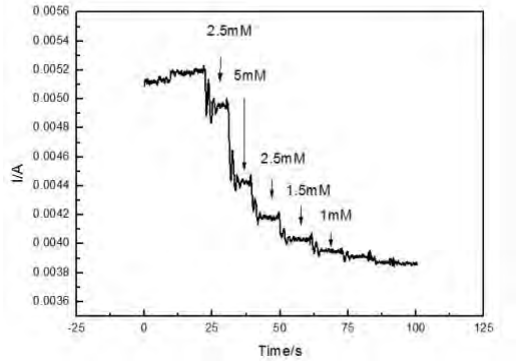

Fig. 8 Amperometric response of the Pd/Ni/Si MCP electrode to successive addition of H_2O_2 at an applied potential of 0.12 V.

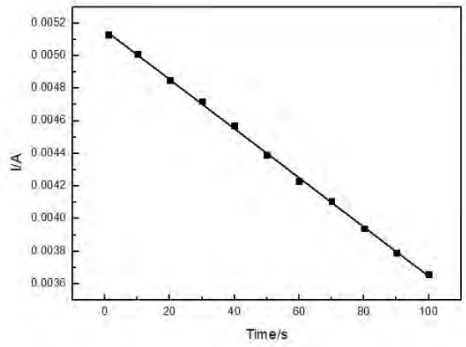

Fig. 9 Calibration curve of the response current as a function of time.

IV. CONCLUSION

In this work, an electrochemical non-enzymatic H_2O_2 sensor based on Pd/Ni/Si MCP electrode is fabricated by electrochemical deposition. The electrode exhibits excellent analytical performance pertaining to the detection of H_2O_2 due to the three-dimensional array of Pd/Ni/Si MCP electrode. It also boasts excellent selectivity, good stability, and outstanding linearity. Our results show that the H_2O_2 sensor based on the Pd/Ni/Si MCP electrode is a promising choice for H_2O_2 detection. The three-dimensional array of Pd/Ni/Si MCP electrode can increase the active sites and enhance the mass transfer of reactants or products, thereby accelerating fast electron transfer and improving the catalytic efficiency.

REFERENCES

[1] H. Razmi, A. Taghvimi, Tin Hexacyanoferrate Nanoparticles Based Electrochemical Sensor for Selective and High Sensitive Determination of H_2O_2 in Acidic Media, Int. J. Electrochem. Sci. 5 (2010) 751-762.

[2] S.S. Khan, E.S. Jin, N. Sojic, P. Pantano, A fluorescence-based imaging-fiber electrode chemical sensor for hydrogen peroxide, Anal. Chim. Acta 404 (2000) 213-221.

[3] A. Tahirovic, A. Copra, E. Omanovic-Miklicanin, K. Kalcher, A chemiluminescence sensor for the determination of hydrogen peroxide, Talanta 72 (2007) 1378-1385.

[4] F. Luo, J. Yin, F. Gao, L. Wang, A non-enzyme hydrogen peroxide sensor based on core/shell silica nanoparticles using synchronous fluorescence spectroscopy, Microchim Acta 165 (2009) 23-28.

[5] W.P Lian, L. W, Y.H Song, H.Z Yuan, S. Zhao, P. Li, L.L Chen, A hydrogen peroxide sensor based on electrochemically roughened siliver electrodes, Electrochim. Acta 54 (2009) 4334-4339.

[6] K.M. Wang, J. Li, X. H. Yang, F.L Shen, X. Wang, A chemiluminescent H_2O_2 sensor based on horseradish peroxidase immobilized by sol-gel method, Sens. Actuators B 65 (2000) 239-240.

[7] S.Q. Liu, H.X. Ju, Renewable reagentless hydrogen peroxide sensor based on direct electron transfer of horseradish peroxidase immobilized on colloidal gold-modified electrode, Anal. Biochem. 207 (2002) 110-116.

[8] A.A. Ansari, P. R. Solanki, B.D. Malhotra, Hydrogen peroxide sensor based on horseradish peroxidase immobilized nanostructured cerium oxide film, J. Biotechnol. 142 (2009) 179-184.

[9] X.M. Chen, J.L. Lin, D. Yuan, P.L. Ci, P.S. Xin, S.H. Xu, L.W. Wang, J. Micromech. Microeng. 18 (2008) 037003.

[10] D. Yuan, P.L. Ci, F. Tian, J. Shi, P.S. Xin, S.H. Xu, L.W. Wang, J. Micro/Nanolith. MEMS MOEMS 8 (2009) 033012.

[11] F.J. Miao, B.R. Tao, L. Sun, T. Liu, J.C. You, L.W. Wang, P.K. Chu, Sens. Actuators B: Chem. 141 (2009) 338.

:

			Natsumi Saito, Yusuke Miura, Takuya Oshima, Masashi Ohkawa, Takashi...
☐	**1164**	4	Thin-Film Vacuum Packaging Based on Porous Anodic Alumina (PAA) for Infrared (IR) Detection *Gwang-Jae Jeon, Woo Young Kim, Hee Chul Lee*
☐	**1198**	4	Characteristics of UV Sensors Using ZnO Nanostructures Synthesized by Galvanostatic Electrochemical Deposition *Tonny Roksana Rashid, Duy-Thach Phan, Gwiy-Sang Chung*
☐	**1257**	3	The Novel Research of Intraocular Pressure Tonometer by Using Inductance Sensor *Yu-Shun Tang, Wei-De Jeng, Ting-Wei Huang, Mang Ou-Yang, Jin-Chern ...*
☐	**1264**	3	Electrical Detection of Norovirus Capsid Using Dielectrophoretic Impedance Measurement Method *Michihiko Nakano, Takafumi Hisajima, Lina Mao, Junya Suehiro*
☐	**1289**	4	Receiver and Amplifier Optimization for Hybrid MOEMS *Wilfried Hortschitz, Jörg Encke, Franz Kohl, Thilo Sauter, Harald S...*
☐	**1331**	4	Optical Fiber Bragg Grating Based Chemical Sensor *David Hsiao-Chuan Wang, Susan Hwang, Simon Maunder, Neil Blenman, J...*
☐	**1342**	4	3D Monolithic Integrated Thermoelectric IR Sensor *Dehui Xu, Bin Xiong, Guoqiang Wu, Yinglei Ma, Errong Jing, Yuelin W...*
☐	**1370**	3	Using the Modified Fiber Membrane to Improve the Efficiency of the Blood Separation in Rapid Test Strip *Chia-Hsien Yeh, Hsin-Zhan Yeh, Yu-Cheng Lin, Pi-Lan Shen*
☐	**1458**	4	Sensing in Sooting Flames: THz Time-Domain Spectroscopy and Tomography *Hamidreza Darabkhani, Miguel Banuelos-Saucedo, John Young, Mark Str...*
☐	**1481**	4	Signal Processing of a High Resolution and Long-Range Displacement Sensor *Neha Arora, Laurent Petit, Muneeb Ullah Khan, Frédéric Lamarque, Ch...*
☐	**1486**	3	Implantable Fiber-Optic SPR Sensor Modified with LPfg and Paa-Ran-Paapba for Continuous Glucose Monitoring *Dachao Li, Peng Wu, Rui Zhu, Jia Yang, Haixia Yu, Kexin Xu*
☐	**1500**	3	Investigation of the Binding Affinity of C-Terminal Domain of SARS Coronavirus Nucleocapsid Protein to Nucleotide Using AlGaN/GaN High Electron Mobility Transistors *You-Ren Hsu, Geng-Yen Lee, Jen-Inn Chyi, Chung-ke Chang, Chih-Cheng...*
☐	**1523**	4	Nano-Size Structure Formation on Si Substrate for Optical Device Application *Daeyoung Kong, Junghwa Oh, Bonghwan Kim, ChanSeob Cho, Jonghyun Lee*
☐	**1704**	3	Real-Time Bio-Sensing Using Micro-Channel Encapsulated Thermal-Piezoresistive Rotational Mode Disk Resonators *Ayesha Iqbal, Jennifer Chapin, Emad Mehdizadeh, Amir Rahafrooz, Byr...*
☐	**1747**	3	A Developed Quantitative Measurement Using the Electro-Microchip for Methamphetamine Detection *Chia-Hsien Yeh, Wei-Ting Wang, Yu-Cheng Lin, Pi-Lan Shen*
☐	**1775**	3	Sub-Population Analysis of Deformability Distribution in Heterogeneous Cell Populations *Il Doh, Young-Ho Cho, Won Chul Lee, Frans Kuypers, Albert Pisano*
☐	**1819**	4	Temperature Sensors Based on D-Shaped Fiber Bragg Grating Coated with Different Thin Films *Chuen-Lin Tien, Li-Chieh Chen, Hsiang-Yi Chiang, Wen-Fung Liu, Hsi-...*
☐	**1984**	4	Highly Sensitive Pressure Sensor Based on Cascaded Long-Period Gratings *Mateusz Smietana, Wojtek Bock, Predrag Mikulic, Jiahua Chen*
☐	**1003**	6	A CMOS Capacitive Micromechanical Oscillator Driven by a Phase-Locked Loop *Hsin-Chih Li, Sheng-Hsiang Tseng, Po-Chiun Huang, Michael Lu*
☐	**1039**	5	Electrostatically Levitated Ring-Shaped Rotational-Gyro/Accelerometer Using All-Digital OFDM Detection with TAD *Tomohito Terasawa, Takamoto Watanabe, Takao Murakoshi*
☐	**1080**	6	A Sensitive Interface Circuit with Wide Dynamic Range for Capacitive Sensors *Fatemeh Aezinia, Behraad Bahreyni*
☐	**1103**	5	A Novel Capacitive Absolute Pressure Sensor Using Son Technology *Xiuchun Hao, Atuhiko Masuda, Kohei Higuchi, Sinya Tanaka, Kazusuke ...*
☐	**1140**	5	Integration of Temperature Detection onto Catheter Flow Sensor for Bronchoscope *Yudai Yamazaki, Kazuhiro Yoshikawa, Mitsuhiro Shikida, Miyoko Matsu...*
☐	**1165**	6	High Performance Humidity Sensors Based on Dopamine Biomolecules Coated Gold-Nanoparticles *Chun-Yi Wang, Ho-Cheng Lee, Che-Hsin Lin*
☐	**1176**	6	A Least Squares Approach for Learning Gas Distribution Maps from a Set of Integral Gas Concentration Measurements Obtained with a TDLAS Sensor *Marco Trincavelli, Victor Hernandez Bennetts, Achim Lilienthal*
☐	**1177**	6	Creating True Gas Concentration Maps in Presence of Multiple Heterogeneous Gas Sources *Victor Hernandez Bennetts, Achim Lilienthal, Marco Trincavelli*
☐	**1231**	5	A Novel Suspension Design for MEMS Sensing Device to Eliminate Planar Spring Constants Mismatch *Kai-Yu Jiang, He-Ling Chen, Wensyang Hsu, Yueh-Kang Lee, Yen-Wu Mia...*
☐	**1322**	5	Simulation and Optimized Design of Capacitance Sensor for Gas/Solid Two-Phase Flow Phase Concentration Measurement *Hongli Hu, Jiebing Yan, Xiaoxin Wang, Xiangxiang Gao*
☐	**1469**	5	Resonance Characteristics of Different Operation Modes of an Orbiting Sphere Viscometer *Stefan Clara, Hannes Antlinger, Bernhard Jakoby*
☐	**1483**	6	A Wireless Irradiance-Temperature-Humidity Sensor for Photovoltaic Plant Monitoring Applications *Alessandro Lazzarini Barnabei, Marco Grassi, Enrico Dallago, Piero ...*

☐	**1490**	5	Measurement of Mixing Ratio and Volume Change of Ethanol-Water Binary Mixtures Using Suspended Microchannel Resonators *Il Lee, Jungchul Lee*
☐	**1522**	6	Hollow Cylindrical Near-Field Electrospining High ß-Phase Crystallisation of Large PVDF Nanofiber Array for Flexible Energy Conversion *Zong-Hsin Liu, Cheng-Teng Pan, Zong-Yu Ou, Wei-Chuan Wang*
☐	**1549**	6	A Compact Impact Sensor Utilizing Elastic Piezoelectric Films and Wide-Bandwidth Amplifier *Jui-Wei Tsai, Jhih-Jhe Wang, Yu-Chuan Su*
☐	**1559**	5	Piezoelectric PDMS Films with Micro Plasma Discharge for Electromechanical Sensors *Jhih-Jhe Wang, Yu-Chuan Su*
☐	**1635**	6	A Novel N x M Array of Resonance-Based Addressable MEMS Actuators *Minfeng Wang, Yang Zhang, Guann-Pyng Li, Mark Bachman*
☐	**1689**	5	Characterization of Paper-Based Flexible Pressure Sensor *Chao-Cheng Shiau, Kan-Chien Li, Zhen-Kai Kao, Ying-Chih Liao, Yen-W...*
☐	**1692**	6	Characterization of Electrical Interferences for Ground Reaction Sensor Cluster *Qingbo Guo, Michael Suster, Rajesh Surapaneni, Carlos Mastrangelo, ...*
☐	**1698**	5	Non-Intrusive Electric Power Sensors for Smart Grid *Pradeep Pai, Lingyao Chen, Faisal Chowdhury, Massood Tabib-Azar*
☐	**1712**	6	Encapsulated Aluminum Nitride SAW Devices for Liquid Sensing Applications *An Tran, Gregory Pandraud, Thomas Moh, Hugo Schellevis, P.M. Sarro,...*
☐	**1719**	5	Flexible Tactile Sensors Based on Nanoimprinted Sub-20 NM Piezoelectric Copolymer Nanograss Films *Alan Chen, Kai-Lun Lin, Chien-Chong Hong, Tong-Miin Liou, Jiann Shi...*
☐	**1845**	5	Calibration-Free Force Sensors Using Liquid Crystal Arrays *Chia-Yi Huang, Liang Lou, Chengkuo Lee*
☐	**1873**	5	Catheter Flow Sensor System and Breathing Measurements in Rabbit *Takuya Matsuyama, Yudai Yamazaki, Takaaki Shikano, Mitsuhiro Shikid...*
☐	**1880**	5	Fabrication and Electrical Characterization of Bottom-Up Silicon Nanowire Resonators *Marc Sansa, Álvaro San Paulo, Francesc Pérez-Murano*
☐	**1948**	5	Poly-SiGe-Based MEMS Xylophone Bar Magnetometer *Véronique Rochus, Roelof Jansen, Harry Tilmans, Xavier Rottenberg, ...*
☐	**2005**	6	Ultra Low Frequency FM Sensing of Piezoelectric Strain Voltage *Anthony Laskovski, Mehmet Yuce, Reza Moheimani*
☐	**2019**	6	Investigation of an Advanced Micro-Inductive Sensor *Paul Köchert, Jens Flügge, Dragan Miletic, Hans-Heinrich Gatzen*
☐	**1170**	7	Room Occupancy Determination with Particle Filtering of Networked Pyroelectric Infrared (PIR) Sensor Data *Takehiro Yokoishi, Jin Mitsugi, Osamu Nakamura, Jun Murai*
☐	**1392**	7	Design of a High-Linearity Up-Conversion Mixer for Wireless Body Area Sensor Network Applications *I-Yu Huang, Wen-Hui Huang*
☐	**1433**	7	Constrained Decentralized Algorithm for the Relative Localization of Wearable Wireless Sensor Nodes *Jihad Hamie, Benoit Denis, Cedric Richard*
☐	**1527**	7	Development of Wireless Communication Methods for Decreasing the Power Consumption of Sensor Nodes *Hironao Okada, Toshihiro Itoh, Takashi Masuda*
☐	**1904**	7	Ultra-Low-Cost Radiation Monitoring System Utilizing Smartphone-Connected Sensors Developed with Internet Community *Yang Ishigaki, Ryo Ichimiya, Yoshinori Matsumoto, Kenji Tanaka*
☐	**2021**	7	Mobile Sensing Systems Based on Improved GDOP for Target Localization and Tracking *Chin-Der Wann*
☐	**2038**	7	RSSI-Based Localization for Wireless Sensor Networks with a Mobile Beacon *Chin-Wei Fan, Yao-Hung Wu, Wei-Mei Chen*
☐	**1053**	8	Fabrication of Microfluidic Neural Probes with in-Channel Electrodes *Dominik Moser, Karsten Seidl, Oliver Paul, Patrick Ruther*
☐	**1820**	8	Fully Back-End TSV Process by Cu Electro-Less Plating for 3D Smart Sensor Systems *Fabio Santagata, Giuseppe Fiorentino, Meng Nie, Catello Farriciello...*
☐	**1935**	8	Assembly of Gold Nanorods for Highly Sensitive Detection of Heavy Metals *Tiziana Placido, Roberto Comparelli, Marinella Striccoli, Angela Ag...*
☐	**1033**	8	FPGA Implementation of a Low-Cost Method for Tracking the Resonance Frequency and the Quality Factor of MEMS Sensors *Farbod Ghassemi, Maira Possas, Gilles Amendola, Jérôme Juillard*
☐	**1042**	8	All Digital Control System for a Novel High Frequency Force Sensor in Non Contact Atomic Force Microscopy *Jeremy Bouloc, Laurent Nony, Christian Loppacher, Wenceslas Rahajan...*
☐	**1606**	8	Structural Health Monitoring Based on AR Models and PZT Sensors *Mario Anderson de Oliveira, Jozué Vieira Filho*
☐	**1678**	8	Patch Type Sensor Module for Diagnosis of Acute Myocardial Infarction *Jihwan Lee, Jaehyo Jung, Donghyuk Shin, Youn Tae Kim*
☐	**1783**	8	Physical Activity Estimation Method by Using Wireless Portable Sensor *Koichi Kurita*
☐	**1829**	8	Investigating Arm Symmetry in Swimming Using Inertial Sensors

			Andy Stamm, Daniel A. James, Rabee M. Hagem, David V. Thiel
☐	**1833**	8	ECG Denoise Method Based on Wavelet Function Learning *Won-Seok Kang, Sanghun Yun, Kookrae Cho*
☐	**1894**	8	Integrated Horizontal ZnO Nanowires for Sensor Applications *Nguyen Quoc Khánh, István Lukács, Sándor Kurunczi, György Sáfrán, Z...*
☐	**1908**	8	Application of KNN Classifier for Acoustic Based Pipe Condition Classification *Zao Feng, Muhammad Tareq Bin Ali, Kirill V. Horoshenkov, Simon Tait*
☐	**1982**	9.5	A Test Structure for in-situ Determination of Residual Stress *Akshdeep Sharma, Deepak Bansal, Kamaljit Rangra, Dinesh Kumar*
☐	**1706**	9.8	Pedestrian Activity Detection in a Multi-Floor Environment by a Smart Phone *Chi-Chung Lo, Yi-Hsiu Chen, Yu-Chee Tseng, Shang-Ming Huang, Yu-Nen...*
☐	**1332**	4	Sandwiched Microfluidic Chip-Based Interferometric Refractometer *Sarun Sumriddetchkajorn, Kosom Chaitavon, Jiti Nukeaw*
☐	**2061**	6	Nonlinear Dynamics of Flying-Height Dependent Magnetic Slider Sensor System in Hard Disk Drives *Jen-Yuan Chang*
☐	**1870**	6	A Piezoelectric Fast Scanning Micromirror with Stiff Symmetrical Lateral-Shift-Free Actuators *Wenjun Liao, Wenjing Liu, Yiping Zhu, Yongming Tang, Baoping Wang, ...*
☐	**2102**	11	Localization Using Dual Orthogonal Stereo Acoustic Sensor Method in Underwater Sensor Networks *Yeon-Mo Yang, Daehee Lee*
☐	**2103**	11	Sub-fF Trimmable Readout Circuit for Tri-Axes Capacitive Microaccelerometers *Hyun Kyu Ouh, Jungryoul Choi, Jungwoo Lee, Sangyun Han, Sungwook Ki...*
☐	**2104**	11	Automated Wire Fault Location Using Impedance Spectroscopy and Genetic Algorithm *Qinghai Shi, Olfa Kanoun*
☐	**2106**	11	Bulk Soil Moisture Estimation Using CosmOz Cosmic Ray Sensor and ANFIS *Ritaban Dutta, Andrew Terhorst, Aaron Hawdon, Bill Cotching*
☐	**2108**	11	Low-Power-Consumption CO2 Gas Sensor Using Ionic Liquids for Green Energy Management *Masahito Honda, Yusuke Takei, Koutarou Ishizu, Hiroshi Imamoto, Tos...*
☐	**2110**	11	A High Performance Microwave Equalizer Based on MEMS Technology *Lei Han, Lei Dong, Yan-Qing Zhu, Li-Feng Wang*
☐	**2122**	11	Highly Sensitive Microelectrode for Glucose Sensing via Inkjet Printing Technology *Pei-Yu Huang*
☐	**2124**	11	Structured Compressive Sensing for Robust and Fast Visual Tracking *Tianxiang Bai, Youfu Li, Jianyang Liu*
☐	**2128**	11	Proposal of Chopper Radar System Enabling Flexible Range Sensitivity Design *Hiromichi Hashizume, Masanori Sugimoto*

Add Selected Papers